THE JOURNAL OF BIOLOGICAL CHEMISTRY VOL. 285, NO. 45, pp. 34537–34548, November 5, 2010

Sorting Motifs of the Endosomal/Lysosomal CLC Chloride Transporters*[S]

Received for publication, July 8, 2010, and in revised form, August 17, 2010 Published, JBC Papers in Press, September 3, 2010, DOI 10.1074/jbc.M110.162545

Tobias Stauber and Thomas J. Jentsch[1]

From the Leibniz-Institut für Molekulare Pharmakologie and Max-Delbrück-Centrum für Molekulare Medizin, Berlin D-13125, Germany

The CLC protein family contains plasma membrane chloride channels and the intracellular chloride-proton exchangers ClC-3–7. The latter proteins mainly reside on the various compartments of the endosomal-lysosomal system where they are involved in the luminal acidification or chloride accumulation. Although their partially overlapping subcellular distribution has been studied extensively, little is known about their targeting mechanism. In a comprehensive study we now performed pulldown experiments to systematically map the differential binding of adaptor proteins of the endosomal sorting machinery (adaptor proteins and GGAs (Golgi-localized, γ-ear containing, Arf binding)) as well as clathrin to the cytosolic regions of the intracellular CLCs. The resulting interaction pattern fitted well to the known subcellular localizations of the CLCs. By mutating potential sorting motifs, we could locate almost all binding sites, including one already known for ClC-3 and several new motifs for ClC-5, -6, and -7. The impact of the identified binding sites on the subcellular localization of CLC transporters was determined by heterologous expression of mutants. Surprisingly, some vesicular CLCs retained their localization after disruption of interaction sites. However, ClC-7 could be partially shifted from lysosomes to the plasma membrane by combined mutation of N-terminal sorting motifs. The localization of its β-subunit, Ostm1, was determined by that of ClC-7. Ostm1 was not capable of redirecting ClC-7 to lysosomes.

The CLC[2] family of chloride transport proteins comprises nine members in mammals (1). Although four of these are plasma membrane-residing chloride channels, the other five, ClC-3–7, localize to distinct, yet partially overlapping compartments of the endo-lysosomal pathway and to other specialized vesicles of the late biosynthetic pathway like synaptic vesicles (1–5). On these organelles, they are involved in enabling luminal acidification and/or chloride accumulation (6–10). Despite the pivotal role of CLC proteins in endo-lysosomal function and their involvement in diverse pathologies in mouse models and human genetic disease (1), little is known about the sorting steps by which they reach their subcellular destinations.

Sorting of endo-lysosomal transmembrane proteins is usually mediated by cytosolic motifs that are recognized by adaptor proteins. These recruit further components of the protein transport machinery, such as clathrin (11, 12). The dileucine motif (DE)*XXX*L(LI) and the tyrosine-based motif Y*XX*Φ (with Φ being a bulky, hydrophobic amino acid) are recognized by the adaptor protein (AP) complexes AP-1–4. The cell uses different APs to recruit cargo proteins for specific transport routes such as AP-2 for endocytosis from the plasma membrane, AP-1 for transport between the *trans*-Golgi network and early endosomes, and AP-3 for sorting from early endosomes and the *trans*-Golgi network to late endosomes (13). The role of AP-4 is less understood. Another sorting signal, which is recognized by adaptors of the Golgi-localized, γ-ear containing, Arf-binding (GGA) family, is the dileucine motif D*XX*LL (14). The three mammalian GGAs mediate sorting at the *trans*-Golgi network by binding to the D*XX*LL motif of cargo and recruiting clathrin for transport to early or late endosomes. It is unclear whether different GGAs (GGA1, -2, -3) are involved in different sorting events (15).

For the predominantly plasma membrane-localized ClC-2, two sorting motifs have been identified, a dileucine motif in the C terminus that recruits AP-1B for sorting to the basolateral membrane of epithelial cells (16) and a tyrosine-based motif in a cytoplasmic loop between helices D and E that mediates recycling between endosomes and the plasma membrane (17). Barttin, the β-subunit of ClC-K channels at the plasma membrane, carries an amino acid sequence (PQPPYVRL) likely to be involved in endocytosis (18). However, it is not clear whether the critical tyrosine belongs to a functional Y*XX*Φ sorting motif or the sequence functions as a so-called PY motif for ubiquitylation-regulated internalization as in the case of the sodium channel ENaC (19). So far no "conventional" AP or GGA binding motifs have been described for intracellular CLCs. ClC-3, which localizes to endocytic compartments (2, 4, 10, 20–23) as well as to synaptic vesicles and synaptic-like microvesicles (2, 3, 24), has been shown to interact via its N terminus with AP-1, AP-2, and clathrin (23). The interaction with clathrin was shown to be dependent on an acidic amino acid stretch with two dileucines, whereas that with AP-2 did not require this stretch. Targeting of ClC-3 to synaptic vesicles and synaptic-like microvesicles has been reported to require AP-3 (3). Various motifs different from AP or GGA interaction sequences

* This work was supported by the Deutsche Forschungsgemeinschaft within the Sonderforschungsbereich SFB 740 (project C5).

[S] The on-line version of this article (available at http://www.jbc.org) contains supplemental Figs. 1–6 and Table 1.

[1] To whom correspondence should be addressed: FMP/MDC, Robert-Rössle-Strasse 10, D-13125 Berlin, Germany. Fax: +49 30 9406 2960; E-mail: Jentsch@fmp-berlin.de.

[2] The abbreviations used are: CLC, a gene family of Cl^- channels and transporters first identified by the cloning of ClC-0 from *T. marmorata*; AP, adaptor protein complex; aa, amino acids; CT, C-terminal domain; NT, N-terminal domain; ER, endoplasmic reticulum; GGA, Golgi-localized, γ-ear containing, Arf-binding (adaptor protein); LAMP-1, lysosome-associated membrane protein-1; TfR, transferrin receptor; AEBSF, 4-(2-aminoethyl)-benzenesulfonyl fluoride; rClC-7, rat ClC-7.

have been shown to be important for the subcellular localization of endo-lysosomal CLCs. A splice variant of ClC-3, ClC-3B, exhibits a PDZ binding motif at its extreme C terminus (25) that recruits ClC-3B to the Golgi complex via an interaction with the PDZ domain-carrying Golgi protein GOPC (26). For ClC-4, which has mostly been reported to localize to endosomes (4, 27) but also to the endoplasmic reticulum (ER) (28), an N-terminal amino acid stretch is reportedly involved in ER retention when expressed heterologously (28). The predominantly endosomal ClC-5 (4, 27, 29–32), a small portion of which is endogenously found also in the plasma membrane (30, 33), bears a C-terminal-located PY motif (34). Although not required for *in vivo* ClC-5 function (33), studies in *Xenopus* oocytes and cultured opossum kidney cells revealed that ubiquitin ligases bind this motif and ubiquitylate ClC-5, stimulating its internalization from the cell surface (34, 35). Although endogenous ClC-6 localizes to late endosomes (36), heterologously expressed ClC-6 has been found on early and recycling endosomes (37). A basic amino acid stretch in ClC-6 seems to be involved in the recruitment of ClC-6 into detergent-resistant membranes that may play a role in its subcellular localization (37). For ClC-7 or its β-subunit Ostm1 (38), no motifs responsible for their lysosomal localization (38–40) have been reported so far. ClC-7 is targeted to lysosomes in the absence of Ostm1, whereas Ostm1 requires ClC-7 to be exported from the ER (38). The aim of this study was to systematically identify the cytosolic sorting motifs of all endosomal/lysosomal CLCs and to investigate their role in subcellular sorting.

EXPERIMENTAL PROCEDURES

Antibodies—For immunoblotting we used mouse monoclonal antibodies directed against the adaptor protein subunits γ (AP-1), β2 and μ2 (both AP-2), δ, μ3A and σ3 (all AP-3), and ε (AP-4) and against GGA2, GGA3 (all from BD Bioscience), α-tubulin (clone DM1A, Sigma), and the rabbit antibody 5A2 against ClC-5 (29). Clathrin heavy chain (CHC) was detected with culture supernatant of the hybridoma cell line X22 (ATCC CRL-2228). HRP-tagged secondary antibodies were purchased from Dianova. For immunostaining of cells, we used monoclonal mouse antibodies directed against transferrin receptor (Invitrogen) and LAMP-1 (clone H4A3, DSHB) and rabbit antibodies against ClC-5 (5A2 (29)), ClC-6 (6N2 (36), 6C3 (41)), ClC-7 (7N4B (40)) and against a C-terminal fusion protein of ClC-0.[3] The latter had not been affinity-purified, which may explain the higher background in non-expressing cells in Figs. 4 and 5. No signal above background staining was observed when constructs not possessing the ClC-0 C terminus had been transfected (not shown). Secondary antibodies conjugated to AlexaFluor 488, 546, or 633 were from Molecular Probes.

Expression Constructs—To generate GST fusion constructs for the C terminus of ClC-7, the sequence between amino acids (aa) 616–805 of human ClC-7 was amplified by PCR and cloned into the expression vector pETM30 (EMBL, protein expression and purification core facility). For the other GST fusion constructs of the CLC N and C termini (NT and CT), respectively, the sequences encoding the following amino acids of the respective human CLC were inserted into pGEX-5X-1 (GE Healthcare) resulting in an N-terminal GST tag: ClC-1-NT, aa 1–117; ClC-1-CT, aa 592–989; ClC-3-NT, aa 1–67; ClC-3-CT, aa 586–760; ClC-4-NT, aa 1–67; ClC-4-CT, aa 584–760; ClC-5-NT, aa 1–54; ClC-5-CT, aa 573–746; ClC-6-NT, aa 1–80; ClC-6-CT, aa 591–869; ClC-7-NT, aa 1–126. For the GST fusion protein of the Ostm1 C terminus, the sequence encoding aa 307–338 of mouse Ostm1 has been cloned into pGEX-5X-1.

For cell culture expression, *Torpedo* ClC-0 (42) was subcloned into pcDNA3 (Invitrogen). Constructs for human ClC-5, human ClC-6, and rat ClC-7 in this vector have been described previously (40, 41). For the generation of chimeric constructs containing parts of ClC-0 and either ClC-6 or ClC-7, the DNA sequences encoding the N-terminal part (aa 1–48 for ClC-0, aa 1–77 for ClC-6, and aa 1–123 for ClC-7), the transmembrane region (43) from the beginning of helix B until the end of helix R (aa 49–524 for ClC-0, aa 78–588 for ClC-6, and aa 124–614 for ClC-7), and the C-terminal region (aa 525–805 for ClC-0, aa 589–869 for ClC-6, and aa 615–805 for ClC-7) of the respective CLC were combined by recombinant PCR with overlapping primers and cloned into pcDNA3. For expression of fluorescently tagged Ostm1, the sequence encoding mouse Ostm1 was cloned into pEGFP-N3 (Clontech) linking Ostm1 with the C-terminal green fluorescent protein (GFP) by the sequence VDGTAGPGSIAT.

To express hClC-5 in *Xenopus* oocytes, the cDNA was cloned into pTLN (44). An HA epitope was inserted between amino acids Glu^{107} and Val^{108} (extra-cytosolic loop between helices B and C) or at the C terminus by PCR mutagenesis. Point mutations were introduced by PCR with primers carrying the respective mutation. All constructs were confirmed by sequencing the complete ORF.

GST Pulldown Assays—GST fusion proteins were expressed in *Escherichia coli* (BL21, DE3) for 5–6 h at 25 °C after induction with 0.12 mg/ml isopropyl-β-D-thiogalactopyranoside before pelleting the cells by centrifugation at 5000 × *g*. Cells were lysed by sonification in PBS supplemented with 0.5 mg/ml AEBSF (Roche Applied Science), protease inhibitor mixture (Complete®, Roche Applied Science), and lysozyme (Sigma) and subsequent incubation with 1% (w/v) Triton X-100 on ice. GST fusion proteins were affinity-purified from a 20,000 × *g* supernatant by a 2-h incubation with glutathione-Sepharose (GE Healthcare) under constant agitation at 4 °C and subsequent washing with PBS. Purity and concentration was estimated by Coomassie staining after SDS-PAGE with BSA as standard.

For a single pulldown experiment, 1.0–1.5 ml of lysate of a 10-cm dish of confluent HeLa cells in PBS supplemented with 1% (w/v) Triton X-100, 0.5 mg/ml AEBSF (Pefabloc SC), protease inhibitor mixture (Complete®), and 1 mM Na_3VO_4 was centrifuged at 10,000 × *g* for 10 min, and the supernatant was incubated with roughly 50 μg of GST fusion protein coupled to Sepharose for 2 h under constant agitation at 4 °C. After 4 washes with PBS, supplemented with 0.1% (w/v) Triton X-100, 0.5 mg/ml AEBSF, and protease inhibitor mixture (Complete®), bound protein was eluted by incubation in SDS sample buffer at 55 °C for 15 min. After sedimenting the Sepharose beads, the

[3] K. Steinmeyer and T. J. Jentsch, unpublished information.

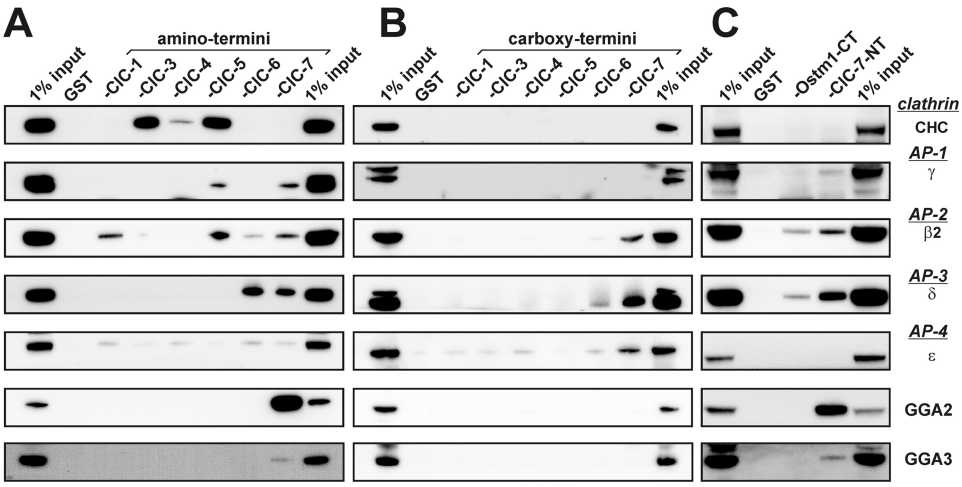

D

		clathrin	AP-1	AP-2	AP-3	AP-4	GGAs	
ClC-1	NT	–	–	+	–	–	–	plasma membrane
	CT	–	–	–	–	–	–	
ClC-3	NT	++	–	–	–	–	–	late endosomes, traffics via plasma membrane
	CT	–	–	–	–	–	–	
ClC-4	NT	+	–	–	–	–	–	early endosomes
	CT	–	–	–	–	–	–	
ClC-5	NT	++	++	++	–	–	–	early endosomes / plasma membrane
	CT	–	–	–	–	–	–	
ClC-6	NT	–	–	(+)	++	–	–	late endosomes (early and recycling endosomes upon ectopic expression)
	CT	–	–	–	+	–	–	
ClC-7	NT	–	+	+	++	–	++	late endosomes / lysosomes (ruffled border)
	CT	–	(+)	+	++	(+)	–	
Ostm1	CT	–	–	+	+	–	–	

FIGURE 1. **Interaction between cytosolic CLC or Ostm1 domains with the sorting machinery.** *A–C*, shown are Western blots of eluates from GST pulldown experiments from HeLa cell lysates with the N-terminal (*A*) and C-terminal (*B*) cytosolic domains of ClC-1 and ClC-3–7 and the C-terminal domain of Ostm1 (*C*). 1% input is shown as the control. Clathrin and adaptor proteins were detected with antibodies against clathrin heavy chain (*CHC*), γ-adaptin (for AP-1), β2-adaptin (for AP-2), δ-adaptin (for AP-3), ϵ-adaptin (for AP-4), GGA2, and GGA3. Ponceau stainings from these pulldown assays showing similar amounts of bait proteins and an immunoblot against α-adaptin (AP-2) are given in supplemental Fig. S1. *D*, shown is a summary of various pulldown experiments from HeLa cell, mouse brain, and kidney lysate as shown in *A–C*. −, no binding detected; (+), not detected in all experiments; +, binding always detected; ++, always strongly detected. The *right column* summarizes the published subcellular localization of the respective CLC.

eluate was separated by SDS-PAGE and probed by immunoblot. Pulldown assays from mouse brain or kidney lysate were performed equivalently, with PBS replaced by HEPES-buffered saline. For tissue lysate preparation, two brains or four kidneys of WT C57Bl/6 mice were homogenized in 10 ml of HEPES-buffered saline with 0.5 mg/ml AEBSF, protease inhibitor mixture (Complete®), and 1 mM Na_3VO_4. The supernatant of a 10-min centrifugation at 10,000 × *g* was supplemented with $1\%_{final}$ Triton X-100. 1.5 ml of the supernatant of 2 further centrifugation steps (15 min at 10,000 × *g* and 20 min at 50,000 × g) was used per pulldown as described above.

Expression in Cell Culture and Fluorescence Microscopy—Plasmid DNA encoding the respective construct was transfected using FuGENE6 (Roche Applied Science) according to the manufacturer's instruction, and cells were grown in a humidified 5% CO_2 incubator at 37 °C for further 24–48 h before fixation with 4% paraformaldehyde in PBS for 15 min. For immunostaining, cells were incubated with 30 mM glycine in PBS for 5 min and permeabilized with 0.1% saponin in PBS for 10 min. Both primary and AlexaFluor-coupled secondary (Molecular Probes) antibodies were applied in PBS, 0.05% saponin supplemented with 3% BSA. Images were acquired with an LSM510 laser scanning confocal microscope equipped with a 63 × 1.4 NA oil immersion lens (Zeiss).

Voltage Clamp Analysis and Surface Expression Assay in Xenopus laevis Oocytes—Capped cRNA was transcribed from constructs in pTLN linearized with MluI (extra-cytosolic HA) or HpaI (C-terminal HA) using the mMessage mMachine kit (Ambion) and SP6 polymerase. 20 ng of cRNA were injected into defolliculated oocytes. Oocytes were kept at 17 °C in ND96 (96 mM NaCl, 2 mM KCl, 1.8 mM $CaCl_2$, 1 mM $MgCl_2$, 5 mM HEPES, pH 7.5) for 2 days before analysis. Two-electrode voltage clamp measurements were performed at room temperature using a TurboTec10C amplifier (npi electronic) and pClamp10 software (Molecular Devices) as described previously (34). Surface expression of HA-tagged ClC-5 protein was determined as described previously (34, 45).

RESULTS

Binding of Endosomal Sorting Machinery to N- and C-terminal Cytosolic Domains of Endosomal/Lysosomal CLCs—To screen for interactions of intracellular CLCs with the endosomal/lysosomal transport machinery, we generated recombinant GST fusion proteins of their cytosolic N- and C-terminal domains (NT and CT, respectively) and of the cytosolic CT of the ClC-7 β-subunit Ostm1, a protein with a single transmembrane span. In addition, we included the cytosolic domains of the plasma membrane-residing channel ClC-1 and GST alone. Pulldown experiments from HeLa cell lysate were performed with equal amounts of the purified, immobilized fusion protein (supplemental Fig. S1). Immunoblotting of bound protein against subunits of all four AP complexes, GGA proteins, and clathrin revealed numerous interactions between the CLC domains and sorting machinery components (Fig. 1). Pulldown experiments from homogenates of mouse kidney and brain yielded similar binding patterns for clathrin and AP complexes (not shown). Interactions with

GGAs, however, could not be probed in those tissues as our antibodies did not recognize the mouse proteins.

ClC-1 interacted through its N terminus with AP-2 (Fig. 1*A*). ClC-3-NT bound clathrin, as reported previously (23). In contrast to this previous study, we did not detect binding of AP-1 or -2 to ClC-3 (Fig. 1*A*). Neither did ClC-3 fusion proteins bind AP-3, as would have been expected from the reported role of AP-3 in targeting ClC-3 (3). ClC-4 bound clathrin weakly with its N terminus (Fig. 1*A*), but no binding to AP or GGA proteins was found with either its N or C terminus (Fig. 1, *A* and *B*). ClC-5-NT pulled down AP-1 and AP-2 as well as clathrin (Fig. 1*A*), whereas none of the investigated proteins was bound by the ClC-5 C terminus (Fig. 1*B*). The N terminus of ClC-6 interacted weakly with AP-2 and more strongly with AP-3 (Fig. 1*A*). AP-3 also bound to the ClC-6 C terminus, albeit less strongly (Fig. 1*B*). Both the N and C termini of ClC-7 bound AP-2 and AP-3 (Fig. 1, *A*–*C*), and its N terminus also bound AP-1 (Fig. 1, *A* and *C*). AP-1 and AP-4 binding to the C terminus of ClC-7 appeared weak because it was not detected in all pulldown assays (compare Figs. 1*B* and 2*G*). The N terminus of ClC-7 also pulled down GGA2 more efficiently than GGA3 (Fig. 1*A*) and GGA1 (not shown). The C terminus of the ClC-7 β-subunit Ostm1 bound AP-2 and AP-3 but not GGA2 or GGA3 (Fig. 1*C*). These interactions were also found when pulldown experiments were performed with lysates of murine adult fibroblasts lacking ClC-7 (39) or Ostm1 (38) (not shown), excluding a possible indirect interaction of Ostm1-CT mediated by bound ClC-7 and vice versa.

Identification of the Sorting Motifs Mediating Clathrin and Adaptor Binding—To investigate the interactions in more detail, we set out to identify the respective binding motifs. The N and C termini of CLCs contain numerous potential tyrosine-based or dileucine sorting motifs that might mediate the binding of APs or GGAs (Fig. 2*A*). To test for the actual role of the potential motifs in intracellular CLCs, we replaced the tyrosines of tyrosine-based motifs and the leucines (or leucine-isoleucines) of dileucine motifs, respectively, by alanines in our GST fusion proteins and tested their impact on adaptor binding in pulldown experiments.

The N-terminal domain of ClC-3, which bound clathrin but not APs or GGAs, contains a potential tyrosine-based motif at Tyr^{27} (^{27}YDDF, Fig. 2*A*). However, previous work (23) showed that clathrin did not bind to this motif but to a more N-terminal stretch containing acidic residues and two dileucines (^{13}LLDLLDE, Fig. 2*A*). Our pulldown experiments confirmed that the strong binding of ClC-3-NT to clathrin (Fig. 1*A*) was virtually abolished when all four leucines of this stretch were replaced by alanines (Fig. 2*B*).

Within the N terminus of ClC-5, which bound AP-1, AP-2 and clathrin, there is one potential tyrosine-based motif at Tyr^{14} (^{14}YDDF). It is conserved in the N termini of ClC-3 and ClC-4 (Fig. 2*A*), which, however, lack detectable AP binding (Fig. 1*A*). We, therefore, initially tested another sequence in ClC-5-NT (ESTWALI^{48}) that almost matches the (DE)*XXX*-L(LI) consensus sequence (Fig. 2*A*). However, mutating Leu^{47} and Ile^{48} to alanines did not significantly reduce the binding of APs and clathrin to ClC-5-NT, whereas, surprisingly, mutating Tyr^{14} to Ala strongly reduced these interactions (Fig. 2*C*). Combining Y14A with the L47A/I48A double mutation did not reduce binding further (Fig. 2*C*).

The N terminus of ClC-6, which bound AP-2 and AP-3 (Fig. 1*A*), contains three potential tyrosine-based motifs (^{48}YESL, ^{61}YLEV, and ^{76}YEAV) (Fig. 2*A*). Because the crystal structure of the prokaryotic EcClC-1 protein suggests that the third motif might extend into the first membrane-spanning helix B (43), we focused on the first two motifs. Mutating Tyr^{48} to Ala strongly reduced AP-2 and AP-3 binding, with a weaker effect seen with the Y61A mutant (Fig. 2*D*). Combining both mutations virtually abolished binding (Fig. 2*D*). Recently, the basic amino acid stretch ^{71}KKGRR (Fig. 2*A*) was implicated in the localization of heterologously expressed ClC-6 to early and/or recycling endosomes, an effect that may involve lipid rafts (37). When this stretch had been mutated to ^{71}AAGAA, ClC-6 was trafficked to late endosomes/lysosomes (37). Introducing this mutation in our GST-ClC-6-NT seemed to affect binding of AP-2 and AP-3 only slightly (Fig. 2*D*).

Despite the low efficiency with which the C terminus of ClC-6 pulled down AP-3 (Fig. 1*B*), it displays many potential sorting motifs (Fig. 2*A*). The EKEDLL^{706} sequence conforms to the (DE)*XXX*L(LI) consensus motif for AP binding, whereas DLTLL^{795} conforms to the D*XX*LL consensus sequence for GGA binding. Both sequences are located in the stretch between the two cystathione β-synthetase domains (46, 47), which is particularly long in ClC-6. In this interdomain stretch there are also three tyrosine-based motifs (^{717}YPNL, ^{774}YAEM, and ^{784}YPDI). Such a motif is also found at the very end of the protein (^{866}YQTI). Another potential Tyr-based motif (^{855}YEFL) is predicted to be positioned within an α-helix of the cystathione β-synthetase 2 domain and is not conserved in mouse (where the Tyr is substituted by Asn). We, therefore, did not investigate it further. We next replaced the key tyrosines and leucines, respectively, of the other motifs by alanines. Mutants in which the extreme C-terminal ^{866}YQTI motif was disrupted (Y866A), either by itself or together with mutations of other potential sorting motifs, did not bind AP-3 anymore (Fig. 2*E*, supplemental Fig. 2*A*). In contrast, various mutants in which the ^{866}YQTI motif was preserved (Fig. 2*E*), even those with all of Leu^{705}-Leu^{706}, Tyr^{717}, Tyr^{774}, Tyr^{784}, and Leu^{794}-Leu^{795} substituted with alanines (supplemental Fig. 2*A*), still pulled down AP-3 similar to the WT C terminus. We conclude that specific binding of AP-3 to the ClC-6 C terminus depends on the ^{866}YQTI motif at the extreme C terminus. In comparison to the N-terminal fusion protein, however, AP-3 binding to ClC-6-CT is weak.

The N terminus of human ClC-7 contains a D*XX*LL consensus sequence for GGA binding (DDELL^{69}) (Fig. 2*A*) that might underlie the binding of GGA2 and GGA3 (Fig. 1*A*). The binding of AP-1, AP-2, and AP-3 might be mediated by the potential (DE)*XXX*L(LI)-type motif EAAPLL^{24} and/or the tyrosine-based motif with ^{94}YESL (Fig. 2*A*). Indeed, mutating leucines Leu^{68} and Leu^{69} to alanines specifically abolished the interaction with the GGA proteins, leaving AP binding unaffected (Fig. 2*F*). Conversely, replacing Leu^{23} and Leu^{24} by alanines abolished the pulldown of APs but not of GGAs. We, therefore, did not examine a putative role of the ^{94}YESL motif in AP binding.

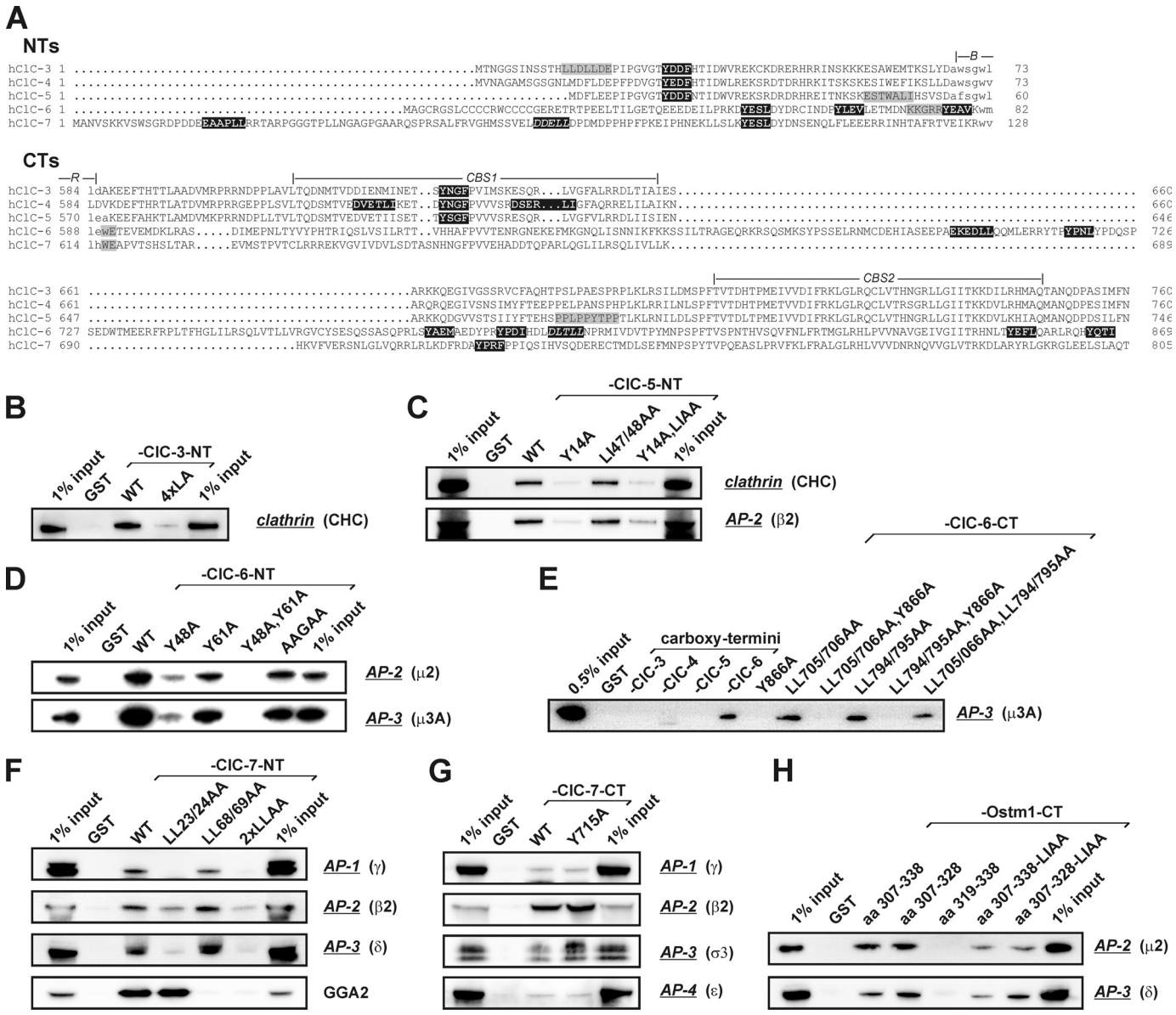

FIGURE 2. **Identification of adaptor protein binding sites.** *A*, shown is a comparison of the N- and C-terminal regions of human ClC-3–7. Residues shown in *lowercase* were not included in the GST fusion proteins. The two conserved cystathione β-synthetase domains and the beginning of helix B and end of helix R are indicated. Potential AP-binding ((DE)*XXX*L(LI) and *YXX*Φ) and GGA binding (D*XX*LL, *italics*) sorting motifs are *highlighted* as *white on a black background*. *Gray boxes* indicate an N-terminal leucine-rich stretch in ClC-3 (23), the N-terminal ESTWALI[48] sequence, and the PY motif in ClC-5 (34), a basic amino acid stretch in the N terminus of ClC-6 (37), and a putative unconventional sorting motif (WE) (49) in the C termini of ClC-6 and -7, respectively. *CHC*, clathrin heavy chain. *B–H*, Western blots of eluates from pulldown experiments explore the binding of interactors identified in Fig. 1 to the respective fusion proteins, either WT or mutants in candidate binding motifs. Eluates from GST columns and 1% (0.5% in *E*) input are shown as controls. For Ponceau staining showing similar amounts of bait protein see supplemental Fig. S2. *B*, clathrin binding to the ClC-3 N terminus is almost abolished when all four leucines of the [13]LLDLL sequence are changed to alanines (*4×LA*). *C*, binding of clathrin and β2-adaptin (AP-2) in a pulldown assay from mouse kidney lysate to the N terminus of ClC-5, a mutant in which Leu[47]-Ile[48] of the ESTWALI[48] sequence was replaced by alanines (*LI47/48AA*) and to mutants in which Tyr-14 of the [14]YDDF motif was changed to alanine either alone (*Y14A*) or in addition to the LI47/48AA mutation (*Y14A/LIAA*). *D*, shown is binding of μ2 (AP-2) and μ3A (AP-3) from mouse brain lysate to the N terminus of ClC-6, either WT or mutants in the [48]YESL and [61]YLEV motifs (*Y48A* and *Y61A*), the double mutant (*Y48A,Y61A*), and the AAGAA mutant in the previously described [71]KKGRR motif (37). *E*, μ3A (AP-3) binding in pulldown from HeLa cell extract with the C termini of ClC-3, -4, and -5 and the ClC-6 C terminus, either WT, the Y866A mutant in the [866]YQTI motif at the extreme C terminus, a mutant (*LL705/706AA*) replacing both leucines of the EKEDLL[706] motif for AP binding by alanines, a similar mutant (*LL794/795AA*) in the DLTLL[795] consensus sequence for GGA binding, and fusion proteins containing these mutations in various combinations. *F*, shown is a pulldown assay from HeLa cell extract with the wild type N terminus of human ClC-7 (*WT*), a mutant with both leucines of EAAPLL[24] changed to alanine (*LL23/24AA*), a similar mutant of the DDELL[69] sequence (*LL68/69AA*), and a mutant combining these mutations (*2×LLAA*). *G*, shown is a pulldown assay from mouse brain lysate with the C terminus of hClC-7, either WT, or a mutant (*Y715A*) in the [715]YPRF[718] motif. *H*, shown is a pulldown assay from HeLa cell extract with the C terminus of Ostm1 (aa 307–338) and various fragments thereof: a membrane-proximal fragment (aa 307–328), an extreme C-terminal fragment (aa 319–338), and mutants changing Leu[318]-Ile[319] to dialanine either in the complete C terminus (*aa 307–338-LIAA*) or in the membrane-proximal fragment (*aa 307–328-LIAA*).

As expected, combined disruption of both dileucine motifs inhibited binding of both APs and GGAs (Fig. 2*F*). The only conventional AP binding motif in the C terminus of ClC-7 is a canonical *YXX*Φ motif at Tyr[715] ([715]YPRF[718], Fig. 2*A*). However, mutating this tyrosine to alanine did not reduce the binding of AP complexes to ClC-7-CT (Fig. 2*G*).

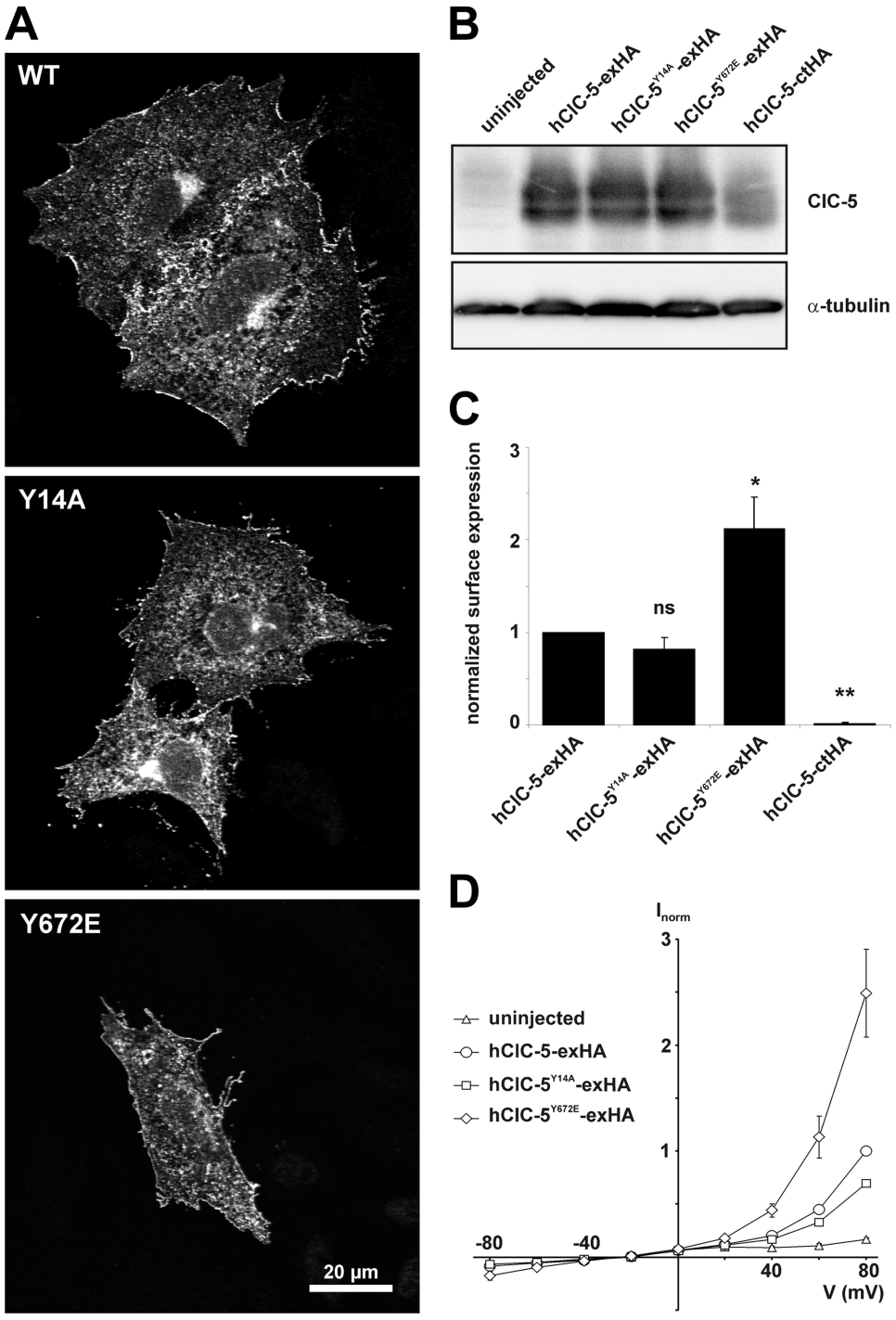

FIGURE 3. **Cell surface expression of ClC-5 mutants.** *A*, subcellular localization in transfected CHO cells of either WT ClC-5 (*top*), a ClC-5 mutant carrying the Y14A mutation in the ^{14}YDDF motif involved in binding AP2 and clathrin, or the Y672E mutation in the PY-motif is shown. Detection used the anti-ClC-5 antibody in immunofluorescence. All constructs show prominent vesicular staining and plasma membrane localization. *B*, an immunoblot against ClC-5 of lysates from *Xenopus* oocytes injected with hClC-5 WT, Y14A, Y672E (all with an extra-cytosolic HA tag), or with hClC-5 carrying an HA-tag at the C terminus (*hClC-5-ctHA*) showed similar expression levels between WT and mutant ClC-5 bearing the extra-cytosolic HA tag. An immunoblot for tubulin served as loading control. *C*, surface expression of HA epitope-tagged hClC-5 (*hClC-5-exHA*) and its mutants Y14A and Y672E in *Xenopus* oocytes were determined in a chemiluminescence assay. hClC-5 carrying an intra-cytosolic, C-terminal HA tag (*hClC-5-ctHA*) served as control. Values are the mean luminescence (±S.E.) normalized to hClC-5-exHA in 5 experiments (9–30 oocytes per construct each). *ns*, non-significant; *, $p < 0.05$; **, $p < 0.001$ compared with hClC-5-exHA by Student's *t* test. *D*, shown are steady-state currents measured by two-electrode voltage clamp of *Xenopus* oocytes injected with cRNA encoding hClC-5 WT, Y14A, or Y672E (all with an extracytosolic HA tag) or uninjected oocytes as control. Values are the mean current ± S.E. normalized to WT at +80 mV (1.56 ± 0.24 μA) from 4 batches of oocytes (2–5 uninjected oocytes and 6–10 oocytes per construct each). *Error bars* are often hidden under the symbol for small S.E.

Although it weakly bound AP-2 and AP-3, the cytosolic C terminus of Ostm1 does not display any consensus tyrosine-based or dileucine motifs. To narrow down the position of the binding site, we generated two overlapping constructs with the first part of the C terminus (Ser^{307}-Thr^{328}) and the extreme C-terminal part (Ile^{319}-Thr^{338}), respectively, both fused to GST. The sequence between Ser^{307} and Thr^{328} was sufficient to pull down AP-2 and AP-3 as efficiently as the full C terminus, whereas no binding to the C-terminal fragment Ile^{319}-Thr^{338} was detected (Fig. 2*H*). The interaction was not dependent on the dipeptide LI^{319} (Fig. 2*H*).

Internalization of Heterologously Expressed ClC-5 Is Largely Independent of Its N-terminal AP-2 Binding Motif—The ^{14}YDDF motif in the N terminus of ClC-5 binds AP-2 (and other adaptors, Figs. 1*A* and 2*C*) and might, therefore, be involved in its endocytosis from the plasma membrane. To test this hypothesis, we introduced the Y14A mutation into a full-length ClC-5 construct and expressed it in CHO cells, which have negligible endogenous levels of ClC-5 (48). Immunofluorescence microscopy did not reveal obvious differences in the subcellular localization between WT and Y14A ClC-5 (Fig. 3*A*). Both proteins displayed some plasma membrane localization in addition to intracellular vesicular staining. We tested whether we could detect stronger plasma membrane staining with a mutant in the C-terminal "PY-like" internalization motif (34) (Fig. 2*A*). This motif mediates E3 ubiquitin ligase-mediated internalization of ClC-5 in heterologous expression systems (34, 35). However, we could not observe an increase in plasma membrane expression of this Y672E mutant by immunofluorescence (Fig. 3*A*).

Even 2-fold increases in plasma membrane expression are difficult to detect by immunofluorescence. For a more reliable, quantitative comparison of cell surface expression between WT and mutants, we

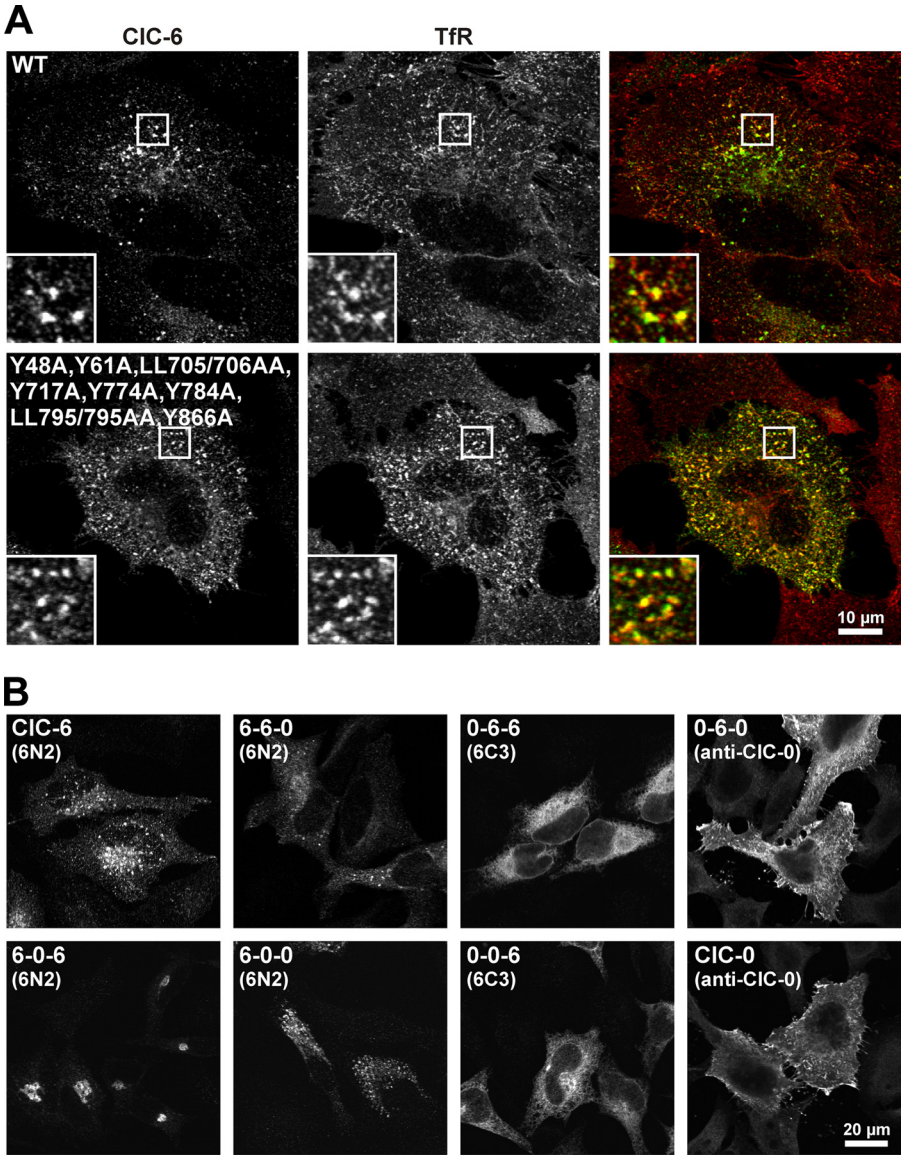

FIGURE 4. **Subcellular sorting of ClC-6.** *A*, shown is immunostaining of HeLa cells transiently transfected with WT ClC-6 (*top panel*) or ClC-$6^{Y48A,Y61A,LL705/706AA,Y717A,Y774A,Y784A,LL795/796AA,Y866A}$ (*lower panel*) for ClC-6 (*green* in merge) and the TfR (*red* in merge). Both ClC-6 proteins colocalize strongly with the TfR (*yellow*). *B*, subcellular localization of chimeras between ClC-6 and ClC-0 in transiently transfected HeLa cells is shown. In chimeras the N terminus (*first number of the name*), the transmembrane region (*second number*), and the C-terminal domain (*third number*) carry the respective parts of ClC-6 (*6*) or ClC-0 (*0*). Immunostaining used antibodies directed against the N terminus of ClC-6 (*6N2*) or the C terminus of ClC-6 (*6C3*) or of ClC-0 (antibodies indicated in *brackets*).

introduced an HA epitope into the extracytosolic loop between helices B and C of ClC-5 (34). As a negative control we appended an HA tag to the cytosolic C terminus. All constructs were expressed to similar extents in *Xenopus* oocytes (Fig. 3*B*). The extracellular presence of the epitope was quantified using an HA antibody in a chemiluminescence assay (34, 45). These experiments revealed that the surface expression of ClC-5^{Y14A} and WT ClC-5 were indistinguishable, whereas the PY mutant ClC-5^{Y672E} showed a roughly 2-fold higher surface expression (Fig. 3*C*) as in our previous work (34). Likewise two-electrode voltage clamp measurements of oocytes expressing the Y672E mutant yielded about 2-fold higher currents than those expressing either WT or Y14A ClC-5 (Fig. 3*D*). We conclude that unlike the C-terminal PQPPYVRL^{675} motif, the N-terminal ^{14}YDDF motif does not play a significant role in plasma membrane localization of ClC-5.

ClC-6 Sorting through Its Cytosolic Domains—To investigate the role of the sorting motifs identified in ClC-6, we compared the subcellular localization of full-length WT with mutant ClC-6 in transfected HeLa cells. As reported previously (37), heterologously expressed ClC-6 colocalized with the recycling-endosome marker transferrin receptor (TfR) (Fig. 4*A*) rather than with markers of late endosomes (not shown). This contrasts with the late endosomal localization of native ClC-6 (36). When the tyrosines of the confirmed AP3-binding ^{866}YQTI motif and of the ^{48}YESL and ^{61}YLEV consensus sequences were changed to alanine either alone or in combination, the localization of the resultant mutant was not altered (not shown). We, therefore, mutated all potential "classical" sorting motifs in the N and C termini of ClC-6 (Fig. 2*A*) in combination. However, even this protein (ClC-$6^{Y48A,Y61A,LL705/706AA,Y717A,Y774A,Y784A,LL794/795AA,Y866A}$) was targeted to TfR-positive endosomes of transfected cells like WT ClC-6 (Fig. 4*A*). We then introduced into this heavily mutated construct two other point mutations (W590A,E591A) to disrupt a potential unconventional sorting signal reported to mediate lysosomal targeting (49). These two residues are located at the end of the last intramembrane helix R and had not been included in the fusion proteins used for pulldown experiments (Fig. 2*A*). However, even these additional mutations did not change the co-localization of ClC-6 with the TfR (not shown).

We finally generated chimeric proteins in which portions of ClC-6 were replaced by equivalent segments of the plasma membrane Cl^- channel ClC-0 from *Torpedo marmorata* (42). Cytoplasmic N-terminal and C-terminal domains and the central transmembrane domain were assembled in different combinations, and their subcellular localization was determined in transfected HeLa cells (Fig. 4*B*). When both the N and C termini of ClC-6 were replaced in chimera 0-6-0 by those of ClC-0, predominant ER-like staining was observed in less than 50% of transfected cells. In the majority of cells the 0-6-0 chimera was strongly plasma membrane-localized just like ClC-0 itself (Fig. 4*B*), demonstrating the importance of the cytosolic domains for

endosomal sorting. Unfortunately, chimeras possessing the ClC-6 C terminus and the N terminus of ClC-0 (0-6-6 and 0-0-6) did not leave the ER (Fig. 4*B*). The two chimeras with an N terminus of ClC-6 and the C terminus of ClC-0 (6-6-0 and 6-0-0) localized to intracellular punctate structures (Fig. 4*B*) where they colocalized with the TfR (not shown) just as heterologously expressed ClC-6. Hence, the N terminus of ClC-6 is sufficient for endosomal targeting. Unexpectedly, the chimera 6-0-6 displayed a perinuclear localization pattern (Fig. 4*B*) and colocalized with the Golgi protein GM130 (supplemental Fig. 3*A*). Disrupting the C-terminal ^{866}YQTI AP-3 binding site of ClC-6 by the Y866A mutation did not affect the apparent ER localization of 0-6-6 and 0-0-6 (not shown) nor the perinuclear localization of 6-0-6 (supplemental Fig. 3*B*) even when combined with mutations Y48A and Y61A, which together virtually abolished binding of AP-2 and AP-3 to the ClC-6 N terminus (Fig. 2*D*).

Sorting Motifs Responsible for the Subcellular Localization of ClC-7/Ostm1—To investigate the role in lysosomal sorting of ClC-7 of identified AP and GGA binding motifs, we transfected HeLa cells with rat ClC-7 (rClC-7) or with chimeras between rClC-7 and ClC-0. We did not cotransfect the β-subunit Ostm1 because Ostm1 bound APs in our pulldown experiments and, therefore, might have confounded our results. Transfected full-length rClC-7 nearly perfectly colocalized with the late endosomal/lysosomal marker protein LAMP-1 (Fig. 5*A*) as observed previously in native cells (40). When we replaced the cytosolic N- and C-terminal regions of rClC-7 by those of ClC-0, the resulting chimera 0-7-0 yielded a predominantly reticular staining pattern indicative of ER retention (Fig. 5*A*). However, a small proportion of 0-7-0 reached the plasma membrane. Unlike WT ClC-7, the chimera did not colocalize with LAMP-1 (Fig. 5*A*).

The N terminus of rClC-7 suffices to direct the plasma membrane Cl^- channel to late endosomes and lysosomes, as revealed by the co-localization of 7-0-0 with LAMP-1 in transfected cells (Fig. 5*B*). When we disrupted in this construct the N-terminal EGAPLL^{24} and DDELL^{67} motifs (homologous to EAAPLL^{24} and DDELL^{69} in human (supplemental Fig. 4), which bind APs and GGAs, respectively (Fig. 2*F*)) either alone (supplemental Fig. 5) or in combination (Fig. 5*B*), the mutant 7-0-0 chimeras were still sorted to late endosomes/lysosomes. Additionally mutating tyrosine Tyr^{92} (homologous to human Tyr^{94} in the YESL^{94} motif that was not involved in AP binding (Fig. 2*F*)) did not alter this localization (supplemental Fig. 5). Compared with human ClC-7, rClC-7 exhibits an additional (DE)*XXX*L(LI) consensus motif (EETPLL^{37}) that is a candidate site for AP protein binding (supplemental Fig. 4). Replacing both leucines of this motif by alanines did not affect the subcellular localization of 7-0-0, whereas the combined disruption of all three N-terminal dileucine motifs brought the 7-0-0 chimera to the plasma membrane (supplemental Fig. 5). Surprisingly, disruption of the GGA binding motif DDELL^{67} was not required for this effect, as also the mutant in which only both consensus sites for AP binding were disrupted ($7^{LL23/24AA,LL36/37AA}$-0-0) reached the cell surface instead of colocalizing with LAMP-1 (Fig. 5*B*).

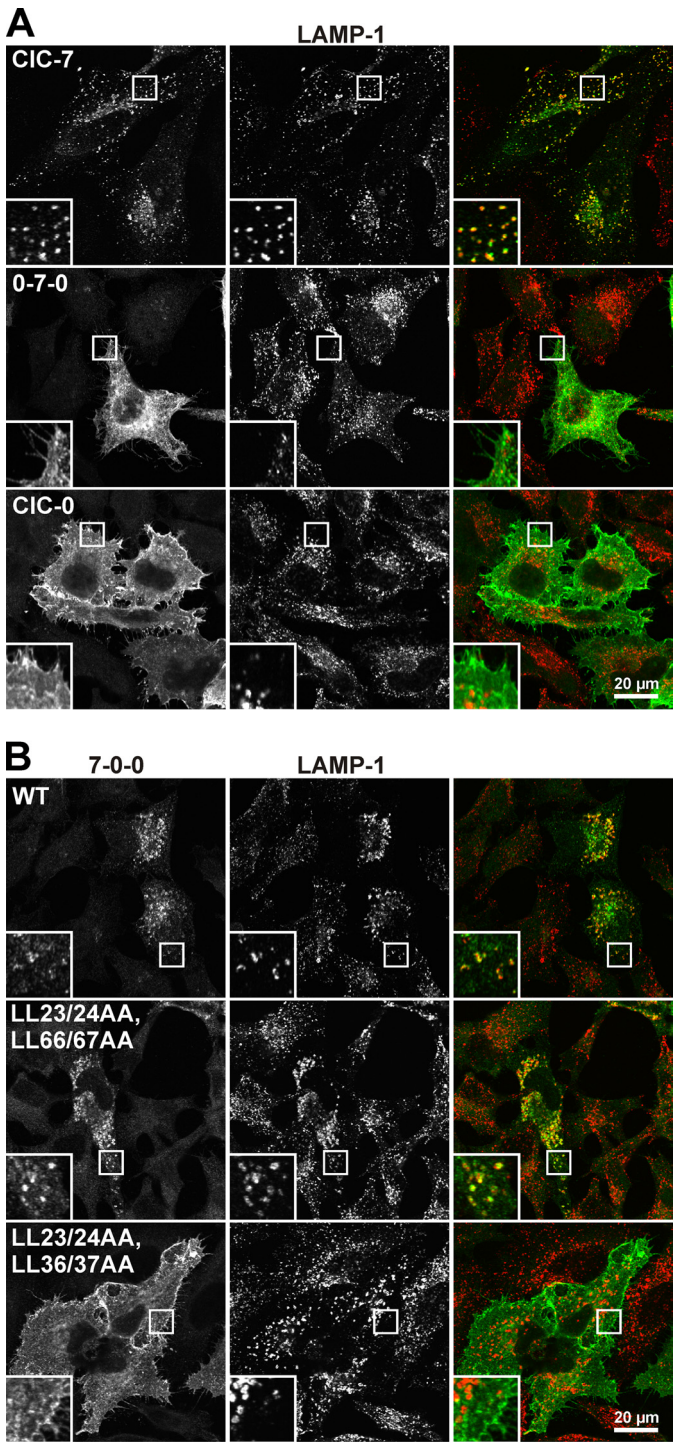

FIGURE 5. **Lysosomal sorting determined by the ClC-7 N terminus.** *A*, subcellular localization of rClC-7 (*top*), a chimera of rClC-7 with N- and C-terminal domains replaced by those of ClC-0 (0-7-0, *below*), and WT ClC-0 (*bottom*) after transient transfection of HeLa cells, in comparison to LAMP-1 as marker for late endosomes and lysosomes. ClC-7 colocalizes with LAMP-1, whereas ClC-0 shows plasma membrane expression. The 0-7-0 chimera shows weak plasma membrane expression in addition to strong ER-like staining. *B*, sorting determinants in the ClC-7 N terminus investigated in HeLa cells transfected with a chimeric protein (7-0-0) in which the N terminus of the plasma membrane channel ClC-0 was replaced by that of rClC-7 (*top panel*) or by ClC-7 N termini carrying two combinations of mutations in the EGAPLL^{24}, EETPLL^{37}, and DDELL^{67} dileucine motifs (EETPLL^{37} present in rat, but not humans). The N terminus of ClC-7 sufficed to target ClC-0 to lysosomes, and combined disruption of the first two motifs in $7^{LL23/24AA,LL36/37AA}$-0–0 resulted in cell surface localization.

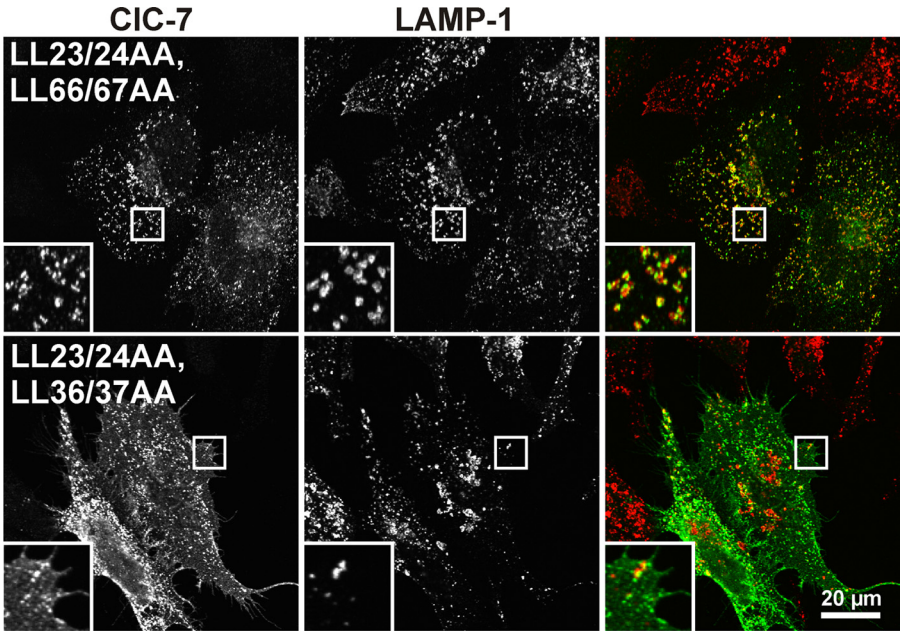

FIGURE 6. **Motifs responsible for the sorting of full-length ClC-7.** HeLa cells fixed 28 h after transient transfection of full-length rClC-7 carrying two combinations of mutations in the EGAPLL[24], EETPLL[37], and DDELL[67] dileucine motifs were immunostained with antibodies against ClC-7 (*green* in merge) and the late endosomal/lysosomal marker LAMP-1 (*red* in merge). Although rClC-7$^{LL23/24AA,LL66/67AA}$ (*upper panel*) almost completely colocalized with LAMP-1 (*yellow*), rClC-7$^{LL23/24AA,LL36/37AA}$-transfected cells (*lower panel*) displayed ClC-7 staining at the plasma membrane in addition to colocalization with LAMP-1.

We next explored the role of these N-terminal dileucine motifs for the targeting of full-length rClC-7. Introducing those mutations that directed the 7-0-0 chimera to the plasma membrane (Fig. 5*B*, supplemental Fig. 5) into rClC-7 resulted in mutants that resided to some extent in the plasma membrane (rClC-7$^{LL23/24AA,LL36/37AA}$ (Fig. 6) and rClC-7$^{LL23/24AA,LL36/37AA,LL66/67AA}$ (supplemental Fig. 6)). In further agreement with results for the 7-0-0 chimera, neither the individual disruption of the three N-terminal dileucine motifs (not shown, supplemental Fig. 6) nor the combined disruption of the EGAPLL[24] and DDELL[67] motifs (Fig. 6) changed the localization of ClC-7.

The remaining partial colocalization of these mutants with LAMP-1 cannot be attributed to signals remaining in the mutated ClC-7 N terminus because these mutations completely abolished the late endosomal/lysosomal localization of the 7-0-0 chimera (Fig. 5*B*). Because the 0-7-0 chimera (Fig. 5*A*) suggests that this localization is not owed to the transmembrane part, it is probably the C terminus, which bound AP adaptors in our pulldown experiments (Fig. 1*B*), that provides additional cues for endosomal/lysosomal sorting. Although disruption of the only tyrosine-based consensus motif (^{715}YPRF^{718}) in the C-terminal GST fusion protein of human ClC-7 did not interfere with binding of APs (Fig. 2*G*), we mutated the homologous Tyr^{713} and Phe^{716} in full-length rClC-7. This mutant (rClC-7$^{YF713/716AA}$) remained localized to late endosomes/lysosomes (supplemental Fig. 6). When this mutation was added on top of those combinations that already partially shifted the constructs to the cell surface, the resulting rClC-7$^{LL23/24AA,LL36/37AA,YF713/716AA}$ (not shown) and rClC-7$^{LL23/24AA,LL36/37AA,LL66/67AA,YF713/716AA}$ (supplemental Fig. 6) still displayed the partial colocalization with LAMP-1 in addition to their presence at the plasma membrane. Obviously the YPRF motif of ClC-7 is not responsible for the apparent ability of the ClC-7 C terminus to partially direct ClC-7 to lysosomes when N-terminal lysosomal trafficking signals have been disrupted.

ClC-7 is required for ER export of its β-subunit, Ostm1, but ClC-7 is targeted to lysosomes even in the absence of Ostm1 (38). As we found weak binding of APs to the ClC-7 β-subunit Ostm1 (Figs. 1*C* and 2H), we wondered whether Ostm1 could support lysosomal sorting of ClC-7 mutants whose dominant lysosomal targeting sequences had been disrupted. To this end, we transiently cotransfected Ostm1 bearing a C-terminal GFP tag (Ostm1-GFP) with either WT or sorting mutants of rClC-7. Coexpression of both WT rClC-7 and rClC-7$^{LL23/24AA,LL36/37AA}$ was sufficient to ensure ER export of Ostm1. In both cases Ostm1-GFP colocalized with the ClC-7 construct (Fig. 7). With WT ClC-7, Ostm1-GFP was sorted to late endosomes/lysosomes, whereas it strongly labeled the cell surface in addition to a partial lysosomal localization when cotransfected with rClC-7$^{LL23/24AA,LL36/37AA}$. Thus, ClC-7 determines the localization of Ostm1.

DISCUSSION

Despite the pivotal role of CLC Cl^-/H^+ exchangers in endosomal/lysosomal function, it has remained enigmatic how their differential localization to the various endosomal/lysosomal compartments is achieved. We used GST fusion proteins of the N- and C-terminal cytosolic domains of all intracellular CLCs to systematically test and compare their interactions with clathrin and its adaptors, AP-1–4 and GGA proteins. The resulting interaction pattern did not depend on the source of cell lysates used for the pulldown assay (HeLa cells, mouse brain, or kidney) and agreed well with the subcellular localization of the various CLC proteins (Fig. 1*D*). For example, AP-3, which mediates cargo sorting for transport to late endosomes, interacted specifically with late endosomal ClC-6 and lysosomal ClC-7/Ostm1, whereas it was not bound by the other CLCs, which localize to earlier endosomal compartments or the plasma membrane. On the other hand, the AP-2 adaptor complex involved in endocytosis from the plasma membrane was strongly bound by ClC-5, which cycles between endosomes and the cell surface.

The amino acid sequences of cytoplasmic CLC domains suggested the presence of consensus binding motifs. In several cases, N- or C-terminal domains displayed more than one candidate binding site. For instance, the N terminus of ClC-7 contains sites for both AP and GGA binding, and the N terminus of

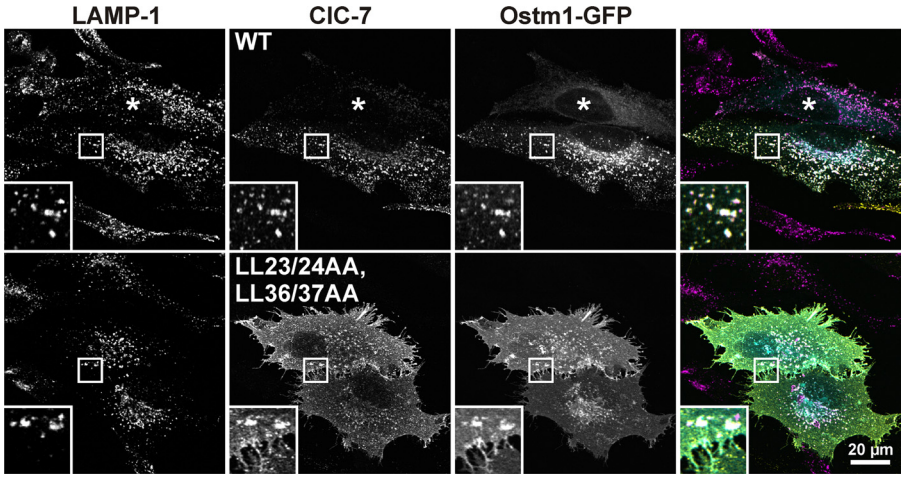

FIGURE 7. **ClC-7-dependent transport of Ostm1.** Subcellular localization of LAMP-1 (*magenta* in merge), ClC-7 (*yellow* in merge) and Ostm1 (*cyan* in merge) in HeLa cells transiently cotransfected with Ostm1-GFP and WT rClC-7 (*upper panel*) or the rClC-7$^{LL23/24AA,LL36/37AA}$ mutant that shows partial cell surface expression (*lower panel*). Although Ostm1-GFP stains an ER-like pattern in cells that do not overexpress ClC-7 strongly (*asterisk*), it colocalizes with ClC-7 to LAMP-1-positive late endosomes/lysosomes in rClC-7-overexpressing cells and with endosomes/lysosomes as well as the plasma membrane in cells expressing rClC-7$^{LL23/24AA,LL36/37AA}$.

ClC-6 displays several sites for AP binding that may be functionally redundant to some degree. Candidate binding sites were validated experimentally by disrupting them through mutagenesis, either individually or in combination. When introduced into the respective fusion protein, these mutations often abolished or reduced binding of adaptor proteins or clathrin, thereby confirming these motifs as being functionally relevant (an overview of these motifs is given in supplemental Table 1). In some cases, however, such mutations failed to affect binding. This situation is not unusual because the candidate binding site might be sterically inaccessible or may require more amino acids than those specified in the consensus sequence. Moreover, even if a "real" binding site had been disrupted by mutagenesis, the functional consequence might be masked by an additional, unidentified binding site in the fusion protein. Indeed, unconventional binding sites do exist, and we were unable to identify the site(s) by which the C termini of either ClC-7 or its β-subunit Ostm1 bound AP-2 and AP-3.

Whereas the binding of specific adaptor proteins to the various CLC transporters agreed well with their intracellular localization (Fig. 1*D*), it often proved difficult to demonstrate their involvement in the intracellular trafficking of CLC proteins. Even when all confirmed adaptor binding sites in the N and C termini of ClC-6 were disrupted by mutagenesis, the heavily mutated ClC-6 was still trafficked to TfR-positive recycling endosomes just like transfected WT ClC-6. One has to realize, however, that this localization is abnormal. Native ClC-6 is found in late endosomes of neurons, the only cells significantly expressing this CLC protein (36). Because the ClC-6 mRNA is rather ubiquitously expressed (50), ClC-6 might require a neuron-specific β-subunit for its stability similar to ClC-K Cl^- channels, which are unstable without their β-subunit barttin (51), or like ClC-7, which needs Ostm1 (38). In contrast to Ostm1, which is not needed for the lysosomal localization of ClC-7 (38), barttin plays a crucial role in targeting ClC-K channels to the plasma membrane (18). Likewise, a so far unknown β-subunit for ClC-6 might traffic ClC-6 to late endosomes. If so, our study addressed a situation that is not found *in vivo*. Nonetheless, the present 6-0-0 chimera showed that the N terminus of ClC-6 contains endosomal targeting signals. Unfortunately, we obtained ambiguous localization results (not shown) when we disrupted the confirmed N-terminal AP binding sites in this chimeric construct. We are, therefore, unable to state with confidence that those motifs play a role in ClC-6 sorting.

The situation is much clearer with the late endosomal/lysosomal ClC-7/Ostm1 heteromer (38). Although AP-1 and AP-2 bound weakly to an unidentified binding site in its C terminus, Ostm1 did not significantly influence the localization of ClC-7 in transfected cells, agreeing with our previous work (38). Even when the disruption of lysosomal sorting signals in ClC-7 led to a partial mislocalization of the transporter to the plasma membrane, co-expression with Ostm1 did not increase the proportion of ClC-7/Ostm1 found in late endosomes/lysosomes. Likewise, and also agreeing with our previous work (38), co-transfection with WT ClC-7 trafficked Ostm1 to late endosomes/lysosomes. Importantly, ClC-7 mutants that mislocalized to the plasma membrane carried Ostm1 to that domain as well. Hence, the subcellular localization of Ostm1 seems to depend entirely on sorting signals in ClC-7, and Ostm1 lacks an effect on ClC-7 trafficking.

Both N and C termini of ClC-7 strongly bound AP-3, an adaptor involved in trafficking to late endosomes. Subsequent transport to lysosomes does not require further sorting. The ClC-7 N terminus also bound GGA proteins, which might direct ClC-7 to early endosomes from where it would be sorted to late endosomes by AP-3. The prominent role in lysosomal sorting of the ClC-7 N terminus was revealed by a chimera in which it replaced the N terminus of the plasma membrane Cl^- channel ClC-0. The resulting chimera 7-0-0 was targeted to late endosomes/lysosomes rather than to the plasma membrane. Strong lysosomal targeting signals are provided by the two dileucine AP-binding motifs present in the rat ClC-7 N terminus. When these two motifs were disrupted together, the mutated 7-0-0 chimera was found in the plasma membrane like ClC-0. Somewhat surprisingly, the GGA binding site did not seem important for lysosomal sorting. Full-length ClC-7 could be partially directed to the plasma membrane by disrupting just those two AP binding motifs. However, a large proportion of the mutant remained in late endosomes/lysosomes to which it was probably directed by its AP-3 binding C terminus. As disruption of the only conventional candidate AP binding site in the C terminus had no effect, we were unable to fully direct ClC-7 to the plasma membrane with a few point mutations. Nonetheless, the partially plasma membrane localized ClC-7 mutant that carries just four point mutations in the cytoplasmic

N terminus should prove useful for characterizing its biophysical properties.

With the notable exception of the N terminus of ClC-5, which bound AP-2 (and clathrin) to a site that we confirmed by mutagenesis, the N and C termini of ClC-3 through ClC-5 did not bind APs or GGAs in our pulldown experiments. Although AP-2 binding to ClC-5 would fit well with the assumed recycling of ClC-5 over the plasma membrane, the disruption of its binding motif did not increase its abundance in the plasma membrane. Hence, other mechanisms must operate in directing these endosomal CLCs to their respective compartments. One such mechanism may be binding to clathrin as described previously for ClC-3 (23). In addition, there might be binding sites in the cytoplasmic aspect of the membrane-spanning parts of CLC proteins, an issue we could not investigate with our pulldown experiments. Indeed, a tyrosine-based motif between intramembrane helices D and E has recently been implicated in the rapid recycling of the Cl^- channel ClC-2 between the plasma membrane and an endosomal compartment (17). On the other hand, ClC-3, -4, and -5 may heterodimerize (4, 52) akin to the previously described heteromer formation between plasma membrane CLC channels (44, 53), and sorting signals present in one of the subunits may determine the trafficking of the heterodimer.

In summary, we newly identified several AP and GGA binding sites in the cytoplasmic parts of vesicular CLC anion/proton exchangers. The known roles of confirmed binding partners in facilitating specific sorting steps agreed well with the native subcellular localization of the CLCs they bound to. In several cases, however, these interactions are not the only ones that direct vesicular CLCs to their normal destination, because no change in localization was observed when the respective binding sites were disrupted. Those cases where vesicular CLC proteins could be directed to the plasma membrane with a few point mutations, however, should provide excellent opportunities to study their biophysical properties in detail.

Acknowledgments—We thank Stephanie Wernick, Janet Liebold, and Patrick Seidler for technical assistance.

REFERENCES

1. Jentsch, T. J. (2008) *Crit. Rev. Biochem. Mol. Biol.* **43,** 3–36
2. Stobrawa, S. M., Breiderhoff, T., Takamori, S., Engel, D., Schweizer, M., Zdebik, A. A., Bösl, M. R., Ruether, K., Jahn, H., Draguhn, A., Jahn, R., and Jentsch, T. J. (2001) *Neuron* **29,** 185–196
3. Salazar, G., Love, R., Styers, M. L., Werner, E., Peden, A., Rodriguez, S., Gearing, M., Wainer, B. H., and Faundez, V. (2004) *J. Biol. Chem.* **279,** 25430–25439
4. Suzuki, T., Rai, T., Hayama, A., Sohara, E., Suda, S., Itoh, T., Sasaki, S., and Uchida, S. (2006) *J. Cell. Physiol.* **206,** 792–798
5. Wartosch, L., Fuhrmann, J. C., Schweizer, M., Stauber, T., and Jentsch, T. J. (2009) *FASEB J.* **23,** 4056–4068
6. Jentsch, T. J. (2007) *J. Physiol.* **578,** 633–640
7. Weinert, S., Jabs, S., Supanchart, C., Schweizer, M., Gimber, N., Richter, M., Rademann, J., Stauber, T., Kornak, U., and Jentsch, T. J. (2010) *Science* **328,** 1401–1403
8. Novarino, G., Weinert, S., Rickheit, G., and Jentsch, T. J. (2010) *Science* **328,** 1398–1401
9. Günther, W., Piwon, N., and Jentsch, T. J. (2003) *Pflügers Arch.* **445,** 456–462
10. Hara-Chikuma, M., Yang, B., Sonawane, N. D., Sasaki, S., Uchida, S., and Verkman, A. S. (2005) *J. Biol. Chem.* **280,** 1241–1247
11. Bonifacino, J. S., and Traub, L. M. (2003) *Annu. Rev. Biochem.* **72,** 395–447
12. Braulke, T., and Bonifacino, J. S. (2009) *Biochim. Biophys. Acta* **1793,** 605–614
13. Robinson, M. S. (2004) *Trends Cell Biol.* **14,** 167–174
14. Bonifacino, J. S. (2004) *Nat. Rev. Mol. Cell Biol.* **5,** 23–32
15. Hirst, J., Sahlender, D. A., Choma, M., Sinka, R., Harbour, M. E., Parkinson, M., and Robinson, M. S. (2009) *Traffic* **10,** 1696–1710
16. Peña-Münzenmayer, G., Catalán, M., Cornejo, I., Figueroa, C. D., Melvin, J. E., Niemeyer, M. I., Cid, L. P., and Sepúlveda, F. V. (2005) *J. Cell Sci.* **118,** 4243–4252
17. Cornejo, I., Niemeyer, M. I., Zúñiga, L., Yusef, Y. R., Sepúlveda, F. V., and Cid, L. P. (2009) *J. Cell. Physiol.* **221,** 650–657
18. Estévez, R., Boettger, T., Stein, V., Birkenhäger, R., Otto, E., Hildebrandt, F., and Jentsch, T. J. (2001) *Nature* **414,** 558–561
19. Staub, O., Gautschi, I., Ishikawa, T., Breitschopf, K., Ciechanover, A., Schild, L., and Rotin, D. (1997) *EMBO J.* **16,** 6325–6336
20. Miller, F. J., Jr., Filali, M., Huss, G. J., Stanic, B., Chamseddine, A., Barna, T. J., and Lamb, F. S. (2007) *Circ. Res.* **101,** 663–671
21. Li, X., Wang, T., Zhao, Z., and Weinman, S. A. (2002) *Am. J. Physiol. Cell Physiol.* **282,** C1483–C1491
22. Weylandt, K. H., Nebrig, M., Jansen-Rosseck, N., Amey, J. S., Carmena, D., Wiedenmann, B., Higgins, C. F., and Sardini, A. (2007) *Mol. Cancer Ther.* **6,** 979–986
23. Zhao, Z., Li, X., Hao, J., Winston, J. H., and Weinman, S. A. (2007) *J. Biol. Chem.* **282,** 29022–29031
24. Maritzen, T., Keating, D. J., Neagoe, I., Zdebik, A. A., and Jentsch, T. J. (2008) *J. Neurosci.* **28,** 10587–10598
25. Ogura, T., Furukawa, T., Toyozaki, T., Yamada, K., Zheng, Y. J., Katayama, Y., Nakaya, H., and Inagaki, N. (2002) *FASEB J.* **16,** 863–865
26. Gentzsch, M., Cui, L., Mengos, A., Chang, X. B., Chen, J. H., and Riordan, J. R. (2003) *J. Biol. Chem.* **278,** 6440–6449
27. Mohammad-Panah, R., Harrison, R., Dhani, S., Ackerley, C., Huan, L. J., Wang, Y., and Bear, C. E. (2003) *J. Biol. Chem.* **278,** 29267–29277
28. Okkenhaug, H., Weylandt, K. H., Carmena, D., Wells, D. J., Higgins, C. F., and Sardini, A. (2006) *FASEB J.* **20,** 2390–2392
29. Günther, W., Lüchow, A., Cluzeaud, F., Vandewalle, A., and Jentsch, T. J. (1998) *Proc. Natl. Acad. Sci. U.S.A.* **95,** 8075–8080
30. Sakamoto, H., Sado, Y., Naito, I., Kwon, T. H., Inoue, S., Endo, K., Kawasaki, M., Uchida, S., Nielsen, S., Sasaki, S., and Marumo, F. (1999) *Am. J. Physiol.* **277,** F957–F965
31. Vandewalle, A., Cluzeaud, F., Peng, K. C., Bens, M., Lüchow, A., Günther, W., and Jentsch, T. J. (2001) *Am. J. Physiol. Cell Physiol.* **280,** C373–C381
32. Wang, Y., Cai, H., Cebotaru, L., Hryciw, D. H., Weinman, E. J., Donowitz, M., Guggino, S. E., and Guggino, W. B. (2005) *Am. J. Physiol. Renal Physiol.* **289,** F850–F862
33. Rickheit, G., Wartosch, L., Schaffer, S., Stobrawa, S. M., Novarino, G., Weinert, S., and Jentsch, T. J. (2010) *J. Biol. Chem.* **285,** 17595–17603
34. Schwake, M., Friedrich, T., and Jentsch, T. J. (2001) *J. Biol. Chem.* **276,** 12049–12054
35. Hryciw, D. H., Ekberg, J., Lee, A., Lensink, I. L., Kumar, S., Guggino, W. B., Cook, D. I., Pollock, C. A., and Poronnik, P. (2004) *J. Biol. Chem.* **279,** 54996–55007
36. Poët, M., Kornak, U., Schweizer, M., Zdebik, A. A., Scheel, O., Hoelter, S., Wurst, W., Schmitt, A., Fuhrmann, J. C., Planells-Cases, R., Mole, S. E., Hübner, C. A., and Jentsch, T. J. (2006) *Proc. Natl. Acad. Sci. U.S.A.* **103,** 13854–13859
37. Ignoul, S., Simaels, J., Hermans, D., Annaert, W., and Eggermont, J. (2007) *PLoS ONE* **2,** e474
38. Lange, P. F., Wartosch, L., Jentsch, T. J., and Fuhrmann, J. C. (2006) *Nature* **440,** 220–223
39. Kasper, D., Planells-Cases, R., Fuhrmann, J. C., Scheel, O., Zeitz, O., Ruether, K., Schmitt, A., Poët, M., Steinfeld, R., Schweizer, M., Kornak, U., and Jentsch, T. J. (2005) *EMBO J.* **24,** 1079–1091
40. Kornak, U., Kasper, D., Bösl, M. R., Kaiser, E., Schweizer, M., Schulz, A., Friedrich, W., Delling, G., and Jentsch, T. J. (2001) *Cell* **104,** 205–215
41. Neagoe, I., Stauber, T., Fidzinski, P., Bergsdorf, E. Y., and Jentsch, T. J.

(2010) *J. Biol. Chem.* **285,** 21689–21697
42. Jentsch, T. J., Steinmeyer, K., and Schwarz, G. (1990) *Nature* **348,** 510–514
43. Dutzler, R., Campbell, E. B., Cadene, M., Chait, B. T., and MacKinnon, R. (2002) *Nature* **415,** 287–294
44. Lorenz, C., Pusch, M., and Jentsch, T. J. (1996) *Proc. Natl. Acad. Sci. U.S.A.* **93,** 13362–13366
45. Zerangue, N., Schwappach, B., Jan, Y. N., and Jan, L. Y. (1999) *Neuron* **22,** 537–548
46. Bateman, A. (1997) *Trends Biochem. Sci.* **22,** 12–13
47. Ponting, C. P. (1997) *J. Mol. Med.* **75,** 160–163
48. Steinmeyer, K., Schwappach, B., Bens, M., Vandewalle, A., and Jentsch, T. J. (1995) *J. Biol. Chem.* **270,** 31172–31177
49. Piccirillo, R., Palmisano, I., Innamorati, G., Bagnato, P., Altimare, D., and Schiaffino, M. V. (2006) *J. Cell Sci.* **119,** 2003–2014
50. Brandt, S., and Jentsch, T. J. (1995) *FEBS Lett.* **377,** 15–20
51. Rickheit, G., Maier, H., Strenzke, N., Andreescu, C. E., De Zeeuw, C. I., Muenscher, A., Zdebik, A. A., and Jentsch, T. J. (2008) *EMBO J.* **27,** 2907–2917
52. Mohammad-Panah, R., Ackerley, C., Rommens, J., Choudhury, M., Wang, Y., and Bear, C. E. (2002) *J. Biol. Chem.* **277,** 566–574
53. Weinreich, F., and Jentsch, T. J. (2001) *J. Biol. Chem.* **276,** 2347–2353